Growth of a Self-Assembled Monolayer by Fractal Aggregation

D. K. Schwartz, S. Steinberg, J. Israelachvili, and J. A. N. Zasadzinski[a]

Department of Chemical and Nuclear Engineering, University of California, Santa Barbara, California 93106

(Received 3 September 1992)

Atomic force microscope images show that self-assembled monolayers of octadecyltrichlorosilane form on mica by nucleating isolated, self-similar domains. With increasing coverage, the fractal dimension of the growing domains evolves from 1.6 to 1.8. At higher coverage, continued growth is limited by adsorption from solution. Monte Carlo simulations that include, for the first time, adsorption as well as surface diffusion qualitatively reproduce both the growth kinetics and evolution of fractal structure much better than a two-dimensional diffusion-limited-aggregation model.

PACS numbers: 68.55.Gi, 68.45.Gd, 81.15.Lm, 82.65.My

Assembling individual molecules into highly ordered "nanostructures" on solid supports [1,2] has important applications in nonlinear optics [3], molecular electronics [4,5], biosensors [6,7], adhesion, and wetting [8,9]. One way to achieve the required organization is by the self-assembly (SA) technique, known [10] to produce monomolecular films of amphiphatic molecules on solid surfaces by spontaneous adsorption [11] from solutions structured by proximity to a boundary [12,13]. Scattering, spectroscopic, and wettability techniques [1], often used to characterize the structure-property relationships of these organic surfaces, average over micron (or larger) scales and thus cannot provide the molecular scale information given by atomic force microscopy (AFM).

Octadecyltrichlorosilane (OTS) self-assembles into a robust monolayer on almost any high-energy surface [11]. By virtue of its hydrolyzable functional groups, OTS molecules can be covalently bound to substrate hydroxyl groups [14] as well as cross-linked within the organosiloxane layer. Although the exposed cleavage plane of mica is a high-energy surface, it is almost entirely chemically nonfunctional [15], making it difficult to form SA monolayers on mica [16,17]. However, steam treating freshly cleaved mica makes it a suitable substrate for OTS monolayer growth, possibly because surface hydroxyl groups are produced [18].

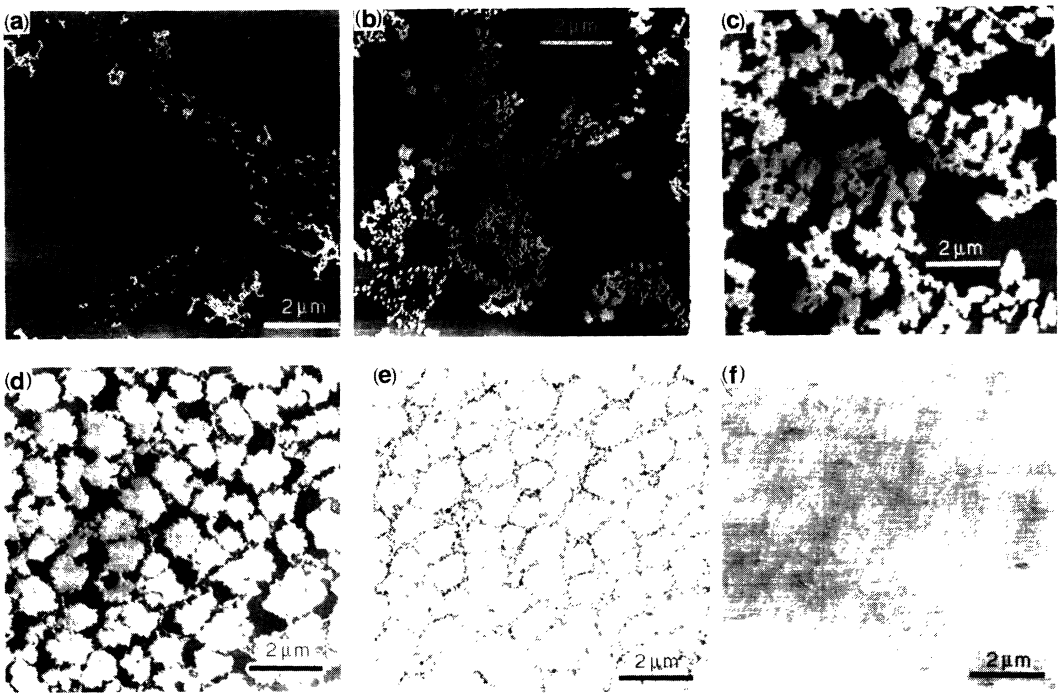

FIG. 1. 10 μm × 10 μm images of partial OTS monolayers immersed for varying amounts of time. Lighter shades represent higher regions, in this case the OTS islands, while the dark background is the mica substrate. The height difference between mica and monolayer is 3.0 ± 0.3 nm, corresponding to a close-packed, untilted OTS monolayer in all cases. (a) After immersion for 0.4 s, small "dots" (88 ± 11 nm diameter) are visible as well as larger aggregates composed of the dots. (b) 2-s immersion: Isolated aggregates are common. (c) 10-s immersion: Aggregates are often touching and becoming less porous. (d) 38-s immersion: Former aggregates are all attached. (e) 66-s immersion: Areas between former aggregates are mostly filled in. (f) 304-s immersion: Although the coverage is complete, faint "scars" indicate the prior gaps between aggregates.

AFM images of mica surfaces exposed for various lengths of time to OTS solutions initially show the formation of isolated islands of close-packed OTS. These islands then serve as centers for aggregation, both for molecules diffusing on the surface, and adsorbing from solution. At low surface coverages, the islands are self-similar with a fractal dimension that increases with surface coverage, suggesting growth primarily via diffusion-limited aggregation. At sufficiently high surface coverage, there is a crossover to growth limited by adsorption from solution. Monte Carlo simulations [19] that include both aggregation by surface diffusion and by adsorption from solution reproduce the coverage kinetics and the evolution of fractal dimension of the monolayer.

Both sides of 1-cm-diam mica disks were cleaved, then exposed to steam for ~ 30 s (until drops formed on the surface), and then dried with clean nitrogen gas. The treated mica disks were immersed in a 0.5-mM solution of OTS in bicyclohexyl for specified amounts of time, and then removed and quickly inserted into a stirred bath of chloroform to remove any remaining unabsorbed OTS and to quench the reaction [20]. After a 2-min rinse the mica disks were dried with nitrogen gas and stored until use (< 14 days). The films were imaged with a Nanoscope II FM [21] in the "height" mode (i.e., utilizing feedback to keep the cantilever at constant deflection and recording sample motion) using a 15-μm scanner and a silicon nitride tip on a cantilever with a spring constant of 0.12 N/m. Typical forces used were on the order of 10 nN. No damage to the films was observed even after multiple scans with the AFM tip.

We obtained at least four images ≥ 10 μm in size from each sample to determine monolayer surface coverage (Fig. 1). After only 0.4 s [Fig. 1(a)], there are many circular dots on the surface; the larger structures [Figs. 1(b) and 1(c)] appear to be aggregates of the dots. These circular dots are surprisingly uniform in size, 88 ± 11 nm in diameter and 3.0 ± 0.3 nm in height (indicative of a close-packed, untilted OTS monolayer), and represent the smallest structures observed, although the resolution limit of the AFM is much less (< 1 nm [22]. These observations confirm that polysiloxane oligomers, formed in the presence of traces of water in solution, adsorb to the surface faster than monomeric trichlorosilanes (or partially hydrolyzed monomers) [23]. At later times (higher surface coverage), the aggregates, whose height remains 3.0 nm, grow by branching and fingering and eventually touch [Figs. 1(b) and 1(c)]. In the final stages, areas between domains fill in and become less porous [Figs. 1(d) and 1(e)]. Even after monolayer formation is complete [Fig. 1(f)], there are slight height deviations showing where gaps had been, suggesting that the final portions adsorbed are less dense or more compressible.

Figure 2(a) shows the surface coverage θ and standard deviations determined from the AFM images for substrates immersed in OTS for various amounts of time. Samples were made on six independent occasions and in several cases more than one sample was made with a similar immersion time to check reproducibility. The relative error in immersion time is ~ 0.3 s. Figure 2(a) clearly shows a crossover (at ~ 5–10 s) between an initial period of fast, linear growth and the subsequent adsorption limited kinetics [$\theta = 1 - \exp(-kt)$].

AFM measurements of surface coverage correlate well with water contact angles, also shown in Fig. 2(a). The stability of the contact angle of water as a function of time is an excellent test of the monolayer tenacity [8]. The advancing contact angles (ϕ_A) on these incomplete OTS monolayers closely follow the surface coverage measured by AFM. The receding contact angles (not shown), although smaller for coverages below 90%, did not depend upon the advancing and receding rates or the resting time of the liquid droplet on the surface after an advance. High values of $\phi_A = 112°$ were obtained for the complete monolayer shown in Fig. 1(f), with no noticeable hysteresis for resting times as long as 10 min. The OTS films are remarkably more stable than Langmuir-Blodgett monolayers or multilayers deposited on mica at similar coverages [8,22].

The shape of the monolayer islands for immersion times of ≤ 10 s appears self-similar [Figs. 1(a)–1(c)]. Figures 3(a) and 3(b) show representative aggregates from films immersed for 3.1 and 6.6 s, respectively. At

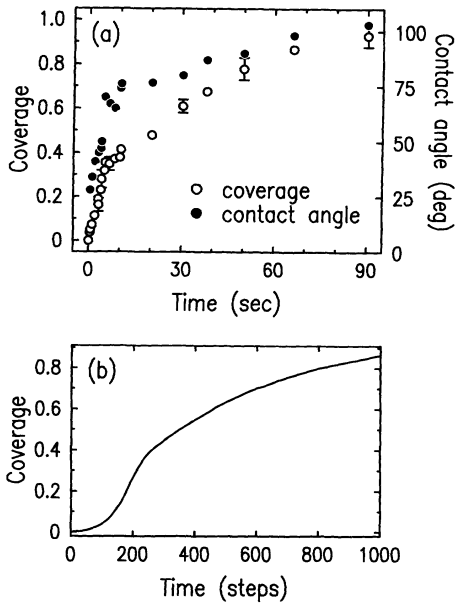

FIG. 2. (a) Film coverage vs time of the OTS monolayer. The first 5 s correspond to fast growth due to DLA. At 5–10 s there is a crossover to absorption-limited growth. (b) Coverage vs time for a simulated monolayer of 35 randomly placed sites on a 140×140 square lattice. The kinetics agree qualitatively with the data in Fig. 2(a) in that there is a crossover between fast DLA and absorption-limited growth. The discrepancy at early times can be explained if $\sim 2\%$ of a monolayer of particles is deposited on the mica as it passes through the air/solution interface.

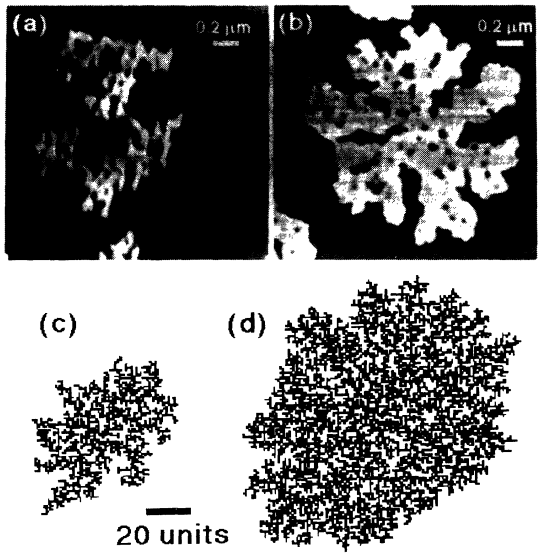

FIG. 3. (a) OTS aggregate taken from a 3.1-s immersion sample. The highly branched, porous structure results in a fractal dimension $D=1.68$. (b) An aggregate from a 6.6-s immersion sample is less branched and some interior holes have been closed off; $D=1.79$. (c) A simulated aggregate grown with an adsorption probability p_a of 0.005 on a 256×256 lattice for 150 time steps. It is highly branched and porous; $D=1.68$. (d) A simulated aggregate after 170 time steps has become less branched and porous ($D=1.79$) although it occupies only a small fraction of the available lattice.

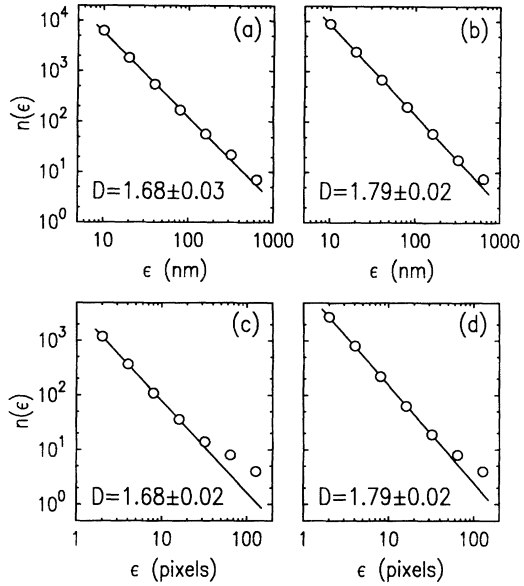

FIG. 4. (a)–(d) Demonstrations of the "box-counting" method for calculating fractal dimension (D) for the aggregates shown in Figs. 3(a)–3(d), respectively. For a mass fractal, the number of boxes of side ε containing a piece of the aggregate, $n(\varepsilon)$, should scale as $n(\varepsilon) \propto \varepsilon^{-D}$ over a range of values of ε. On the log-log plots shown, therefore, the data should form a straight line, and the lines show the best fit by a line over the range for which $n(\varepsilon) \geq 20$.

least six such aggregates from each sample were analyzed and the fractal dimension (D) for each was calculated using the "box-counting" method [24]. The number of boxes of size ε which contain portions of the aggregate, $n(\varepsilon)$, scales as $n(\varepsilon) \propto \varepsilon^{-D}$. Plots of $n(\varepsilon)$ versus ε for the aggregates in Figs. 3(a) and 3(b) are shown in Figs. 4(a) and 4(b). The results were averaged for each film and are summarized in Fig. 5(a). The fractal dimension of the aggregates, D, increases from 1.60 to 1.79 with increasing surface coverage.

The two regimes of growth kinetics [Fig. 2(a)] are directly linked to the partial monolayer structure. Initially (<10 s), the monolayer consists of branched aggregates reminiscent of two-dimensional diffusion-limited aggregation (DLA) [24]. At higher surface coverage, domains are less porous and begin to touch. The fractal dimension of the aggregates shows a corresponding increase from about 1.6 to 1.8 with surface coverage. At this point, the coverage kinetics slows and $\theta \approx [1 - \exp(-kt)]$, suggesting that growth is limited by adsorption from solution. We have modeled this process by computer simulations which combine conventional two-dimensional DLA with a probability of adsorption from solution. The simulation was carried out on a square lattice using a Monte Carlo algorithm [19]. In a given time step, any unattached particle on the surface was capable of diffusing to an adjacent unoccupied site, as in DLA. However, all unoccupied sites also had an adsorption probability (p_a) of becoming occupied by a particle (from solution); the adsorbed particle was then capable of diffusion in subsequent time steps. If a particle diffused or adsorbed next to a site that was part of an attached aggregate, it became part of that aggregate. We estimated p_a as the number of OTS oligomers in solution [equivalent in volume to the 90-nm-diam monolayer "dots" observed in Fig. 1(a)] arriving at a site on the mica surface in the time necessary for diffusion of the oligomer by one dot diameter (the size of a site in the simulation) on the mica surface. The diffusion of the oligomer by one diameter on the surface defined the time step in the simulation. For reasonable values of the experimental parameters, p_a ranges from 0.001 to 0.02.

Figure 2(b) shows the coverage kinetics of 35 randomly placed aggregates growing on a 140×140 lattice with $p_a=0.002$. Changing the absorption probability p_a simply scales the time axis and has no qualitative effect on coverage kinetics or aggregate shape. Qualitatively, the simulation captures the important features of the experiment, i.e., the crossover between fast growth related to DLA and adsorption-limited kinetics at later times or higher coverages. However, in the simulation, there is an induction period where the coverage is very low, which is not present in the experimental data. This is the time required for the surface to collect sufficient diffusing particles for aggregate nucleation. We speculate that in the experiment, sufficient particles adsorb on the mica during its pass through the air/solution interface to eliminate the

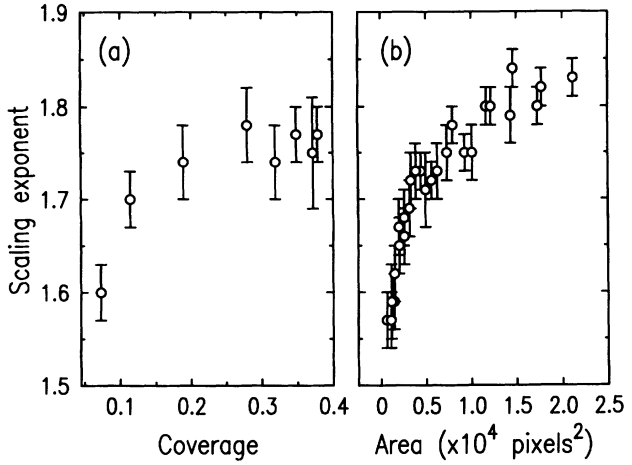

FIG. 5. (a) The average box-counting fractal dimension (D) for all aggregates analyzed for a given immersion time. At least six aggregates contributed to each average. A trend of increasing D with coverage (or time) can be clearly seen. (b) Box counting D for simulated aggregates grown in a variety of conditions, with values of p_a ranging from 0.001 to 0.01, and on lattices ranging in size from 128×128 to 512×512. The crossover in D always correlated simply with aggregate area (mass), implying that the competition between diffusive growth and absorption-limited growth depends simply on aggregate size.

start-up period.

Figure 3(c) shows a typical simulated aggregate in the highly branched early regime, while Fig. 3(d) shows a simulated particle during the later stages of growth. The box-counting data for the respective simulated aggregates are shown in Figs. 4(c) and 4(d). The evolution of the scaling exponent in the simulations, shown in Fig. 5(b), is insensitive to particular values of p_a or lattice size. The crossover in scaling exponent always depends simply on surface coverage. This means that the crucial factor in both simulation and experiment is the competition between two-dimensional diffusers and "three-dimensional" adsorbers. At low surface coverage, the odds of a particle adsorbing from solution inside an aggregate perimeter is negligible, so the aggregate takes on the highly branched structure and low fractal dimension characteristic of two-dimensional DLA [24]. In our experiment, however, particles can adsorb inside the aggregate, and as surface coverage increases, this occurs with increasing probability.

We have identified two distinct growth mechanisms which account for the kinetics of silanation of atomically smooth mica surfaces. Monolayer growth of OTS on mica occurs by nucleation and growth of self-similar islands and is significantly different from the uniform growth observed on silicon [25]. We have also shown that two-dimensional diffusion-limited aggregation supplemented by random adsorption of OTS oligomers from solution can qualitatively describe both the coverage kinetics and the structure of the partial monolayers. The structure of partially formed monolayers is of importance, since it should help us understand the mechanism of monolayer formation and establish a protocol to construct reproducible, closely packed, complete monolayers.

This work was supported by ONR Grant No. N00014-90-J-1551, NSF Grant No. CTS90-15537, NIH Grant No. GM 47334, the Donors of the Petroleum Research Foundation, and DOE Grant No. DE-FG03-87ER45331. The authors acknowledge discussions with H. Weinberg, B. Meng, M. Goulian, and J. Sagiv.

[a]To whom correspondence should be addressed. Electronic address: gorilla@squid.ucsb.edu FAX: 805-893-4731.

[1] J. D. Swalen *et al.*, Langmuir **3**, 932 (1987).
[2] J.-M. Lehn, Angew. Chem. Int. Ed. Engl. **29**, 1304 (1990).
[3] S. K. Kurtz, *Quantum Mechanics: A Treatise*, edited by H. Rubin and C. L. Tang (Academic, New York, 1975), Vol. 1-B, Chap. 3.
[4] J. J. Hopfield, J. N. Onuchic, and D. N. Beratan, Science **241**, 817 (1988).
[5] S. Palacin, A. Ruandel-Teixier, and A. Barraud, Mol. Cryst. Liq. Cryst. **156**, 331 (1988).
[6] I. Rubinstein *et al.*, Nature (London) **332**, 426 (1988); **337**, 217 (1989).
[7] H. Dugas, *Bioorganic Chemistry, a Chemical Approach to Enzyme Action* (Springer-Verlag, New York, 1989), 2nd ed.
[8] Y. L. Chen, C. A. Helm, and J. Israelachvili, J. Phys. Chem. **95**, 10736 (1991).
[9] P.-G. de Gennes, Rev. Mod. Phys. **57**, 827 (1985).
[10] W. C. Bigellow, D. L. Pickett, and W. A. Zismann, J. Colloid Sci. **1**, 513 (1946).
[11] R. Maoz and J. Sagiv, J. Colloid Interface Sci. **100**, 465 (1984).
[12] D. Mobius, Ber. Bunsen-Ges. Phys. Chem. **82**, 848 (1978).
[13] J. Van Alsten and S. Granick, Phys. Rev. Lett. **61**, 2570 (1988).
[14] E. P. Pluedmann, Silane Coupling Agents (Plenum, New York, 1982).
[15] R. M. Barrer, *Zeolites and Clay Minerals as Sorbents and Molecular Sieves* (Academic, London, 1978).
[16] G. A. Carson, M.S. thesis, University of Illinois, 1989.
[17] C. R. Kessel and S. Granick, Langmuir **7**, 532 (1991).
[18] N. Tillman *et al.*, J. Am. Chem. Soc. **110**, 6136 (1988).
[19] *Monte Carlo Methods in Statistical Physics*, edited by K. Binder (Springer-Verlag, Berlin, 1986), Vol. 7.
[20] Aldrich Chemical Co., Milwaukee, Wisconsin.
[21] Digital Instruments, Inc., Goleta, CA 93117.
[22] D. K. Schwartz *et al.*, Science **257**, 508 (1992).
[23] A. Ulman, *An Introduction to Ultrathin Organic Films from Langmuir-Blodgett to Self-Assembly* (Academic, San Diego, 1991).
[24] P. Meakin, in *Phase Transitions and Critical Phenomena*, edited by C. Domb and L. Lebowitz (Academic , London, 1988), Vol. 12; *The Fractal Approach to Heterogeneous Chemistry*, edited by D. Avnir (Wiley, New York, 1989).
[25] S. R. Wasserman *et al.*, J. Am. Chem. Soc. **111**, 5852 (1989).

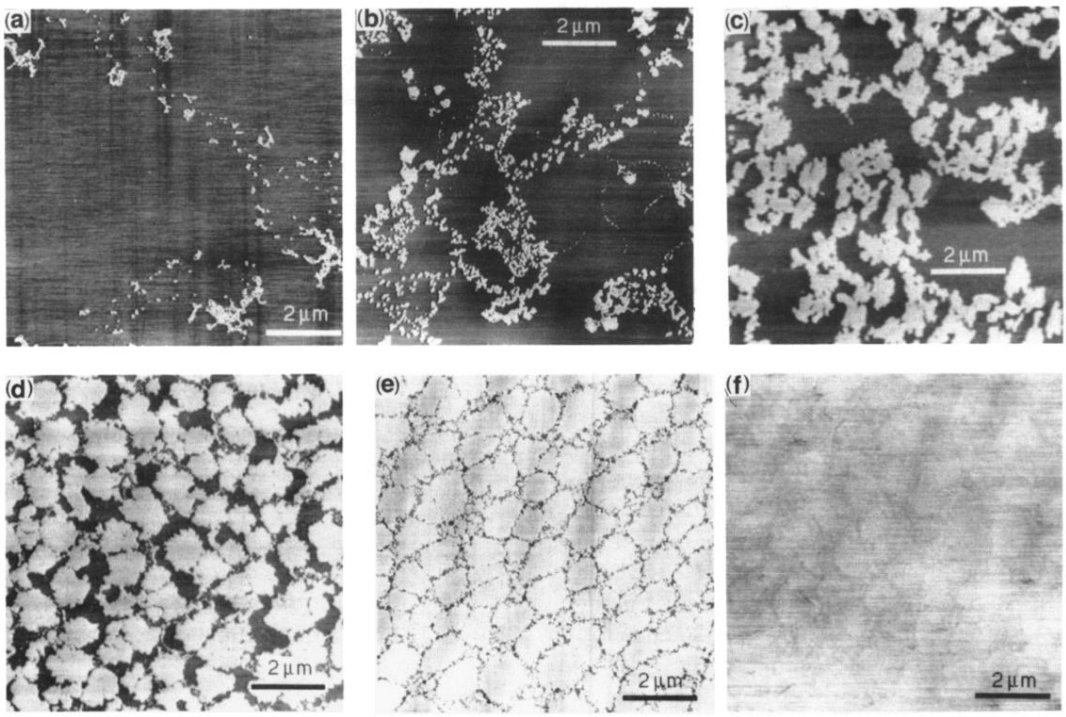

FIG. 1. 10 μm × 10 μm images of partial OTS monolayers immersed for varying amounts of time. Lighter shades represent higher regions, in this case the OTS islands, while the dark background is the mica substrate. The height difference between mica and monolayer is 3.0 ± 0.3 nm, corresponding to a close-packed, untilted OTS monolayer in all cases. (a) After immersion for 0.4 s, small "dots" (88 ± 11 nm diameter) are visible as well as larger aggregates composed of the dots. (b) 2-s immersion: Isolated aggregates are common. (c) 10-s immersion: Aggregates are often touching and becoming less porous. (d) 38-s immersion: Former aggregates are all attached. (e) 66-s immersion: Areas between former aggregates are mostly filled in. (f) 304-s immersion: Although the coverage is complete, faint "scars" indicate the prior gaps between aggregates.

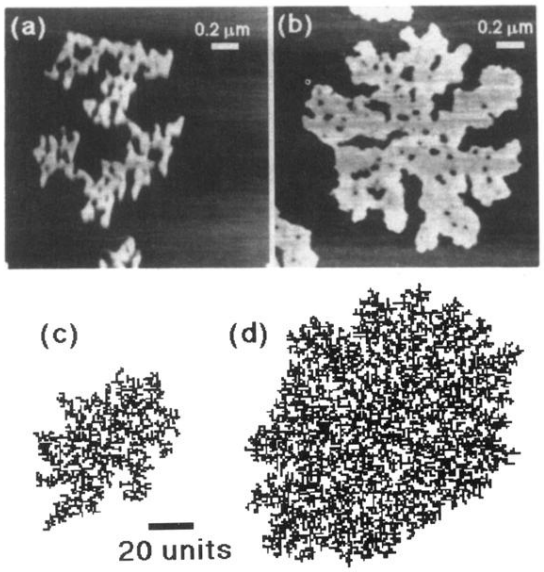

FIG. 3. (a) OTS aggregate taken from a 3.1-s immersion sample. The highly branched, porous structure results in a fractal dimension $D=1.68$. (b) An aggregate from a 6.6-s immersion sample is less branched and some interior holes have been closed off; $D=1.79$. (c) A simulated aggregate grown with an adsorption probability p_a of 0.005 on a 256×256 lattice for 150 time steps. It is highly branched and porous; $D=1.68$. (d) A simulated aggregate after 170 time steps has become less branched and porous ($D=1.79$) although it occupies only a small fraction of the available lattice.